08.3

Flexible Solar Cells Based on GaAs/AlGaAs Heterostructure with Improved Weight and Dimension Characteristics

© A.S. Goltaev[1], A.A. Vorobyov[1], A.M. Mozharov[1], A.V. Pavlov[1], D.M. Mitin[1,2], V.V. Fedorov[1,2], Yu.S. Berdnikov[1], I.S. Mukhin[1,2]

[1] Alferov Federal State Budgetary Institution of Higher Education and Science Saint Petersburg National Research Academic University of the Russian Academy of Sciences, St. Petersburg, Russia
[2] Peter the Great Saint-Petersburg Polytechnic University, St. Petersburg, Russia
E-mail: akbapnym@yandex.ru

Received May 6, 2022
Revised July 25, 2022
Accepted July 25, 2022

In this work, we propose and realize new design strategies for flexible solar cells based on the classical GaAs/AlGaAs heterojunction. The InAlP layer was chosen as a sacrificial layer for lift-off process in order to separate the heterostructure from the substrate, we also used poly (methyl methacrylate)membrane as a flexible substrate. The combination of these design strategies made it possible to achieve relativley high specific power — 778 W/kg.

Keywords: solar cell, GaAs, ELO, flexible electronics.

DOI: 10.21883/TPL.2022.09.55081.19245

Solar power engineering is the most promising line of development of renewable energy resources. Heterostructures based on GaAs with direct band gap with direct band gap rank among the leaders in efficiency in the class of single-junction solar cells (SCs) [1]. The mechanical properties of thin layers of semiconductor $A^{III}B^{V}$ compounds are sufficient for their application in flexible SCs integrated into wearable electronics, portable devices, automated cars and, and drones [2]. In fact, record-high efficiencies of GaAs-based SCs were obtained exactly for flexible lift-off SCs the growth substrate [3]. In addition, ultrathin and highly efficient GaAs-based SCs have been demonstrated recently [4].

The required flexibility and lightness of SCs preclude one from resorting to various traditional solutions and stimulate the search for novel designs of transparent electrodes and support layers compatible with flexible absorbing $A^{III}B^{V}$ heterostructures. Flexible carriers are needed in order to fabricate and utilize an SC lifted off the growth substrate. Various materials (e.g., thin metal foils or organic polymers) may serve as such carriers. Although metal foils have a number of advantages, such as high electric and thermal conductivity values and thermal and radiation resistance, their high density contributes to an increase in mass of the end product.

In the present study, we report the results of modeling of the classical single-junction SC design with the highest efficiency and the results of synthesis and examination of photovoltaic parameters of a flexible SC based on a GaAs/AlGaAs heterostructure lifted off the growth substrate. InAlP was used as a sacrificial layer for lifting the heterostructure off the growth substrate. A polymethyl methacrylate (PMMA) membrane, which provides both the needed mechanical flexibility and a high power/mass ratio of an SC, was proposed to be used as a transparent flexible carrier.

Numerical modeling of the SC operation modes was performed in order to determine the optimum composition of layers of a lift-off SC corresponding to the highest possible efficiency. The absorption of light in the semiconductor GaAs/AlGaAs heterostructure and the carrier separation as a function of the composition, thickness, and doping level of SC layers were taken into account in this modeling. The propagation and absorption of light in the heterostructure were examined in the wave optics approximation, and the photocell operation was analyzed using the semiconductor drift–diffusion model with Fermi–Dirac carrier statistics. The classical geometry of a GaAs/AlGaAs SC with a single $p-n$ junction was examined (see the composition and description of layers in the inset of Fig. 1, *b*). The optical and semiconductor material parameters were taken from [5,6]. Both modeled contacts were regarded as ideal Ohmic ones. Additional antireflective coatings were not introduced into the model.

At the first stage, the transport of photogenerated carriers through wide-band SC barriers was examined in order to determine the voltage drop across them as a function of layer composition, type, and doping level. It was found that a *p*-type barrier ensures the flow of photocurrent with negligible voltage losses in the entire range of compositions and is well-suited for the formation of a wide-band SC window within which the optical losses need to be minimized. In contrast, an *n*-type barrier produces significant voltage losses in compositions with more than 40% of aluminum, and doping impurity densities in excess of $5 \cdot 10^{18}$ cm^{-3} are needed to use it as a bottom potential barrier of an SC.

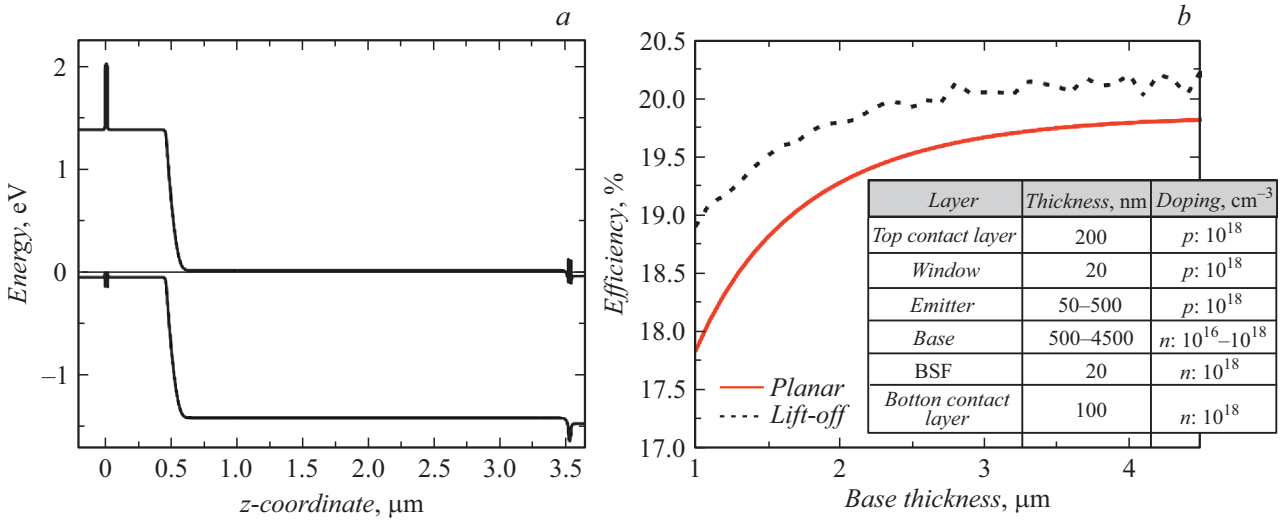

Figure 1. *a* — Band diagram of an SC with an emitter 500 nm in thickness and a base with a thickness of 3 μm. *b* — SC efficiency before and after lift-off. The composition of SC layers is presented in the inset.

Figure 2. Optical image of the flexible SC on a polymer carrier.

At the second stage, the thickness and the doping level of the base and the thickness of the emitter layer were varied. The doping level of the emitter layer was fixed at $10^{18}\,\mathrm{cm}^{-3}$, which is the highest value that does not induce any significant reduction in the lifetime of minority carriers. The thickness and the doping level of both barriers were set to 20 nm and $10^{18}\,\mathrm{cm}^{-3}$. A *p*-type AlGaAs barrier with an aluminum content of 80% was chosen to be used as a wide-band window. The aluminum content of the bottom potential barrier layer was 20%. Operation modes of the photocell under external illumination with the AM1.5G spectrum and under a voltage of 0–1.2 V varying in 10 mV increments were numerical calculation to estimate the efficiency of the structure. The sought-for estimate was obtained by analyzing I–V curve and finding the voltage that corresponds to the highest power. This numerical calculation that the optimum doping level of the base falls within the $6 \cdot 10^{16}-3 \cdot 10^{17}\,\mathrm{cm}^{-3}$ range, and the emitter layer thickness is 500 nm.. Figure 1, *a* shows the band diagram of an SC with a base thickness of 3 μm. Figure 1, *b* presents the results of numerical modeling of the dependence of the SC efficiency (without an antireflective coating) on the base thickness before and after lifting off the growth substrate [7]. It can be seen that, following lift-off SC and the formation of a metal contact on the back surface, the photocell operation efficiency increases by $0.3 \pm 0.1\%$ due to the additional absorption of light reflected from the bottom contact.

A Veeco GEN-III molecular beam epitaxy system was used to form SC heterostructures based on GaAs and AlGaAs and InAlP (sacrificial layer) solid solutions. Epitaxial Si-doped *n*-type $n_n \sim 10^{18}\,\mathrm{cm}^{-3}$ (001) GaAs wafers with a diameter of 50 mm were used as substrates

A top mesh contact was formed next by contact photolithography. By vacuum thermal evaporation Cr/Au layers (5nm/150nm) were deposited. Local selective wet etching was performed to remove the contact GaAs layer.

A PMMA layer 20 μm in thickness, which was deposited using the spin coating method with subsequent thermal treatment for polymerization, served as the carrier material. The sacrificial InAlP layer was etched in a solution of hydrochloric (5%) and orthophosphoric (85%) acids at room temperature. Following lift-off of the thin-film SC heterostructure, a low-temperature continuous *n*-type bottom contact was formed, since polymer carriers limit

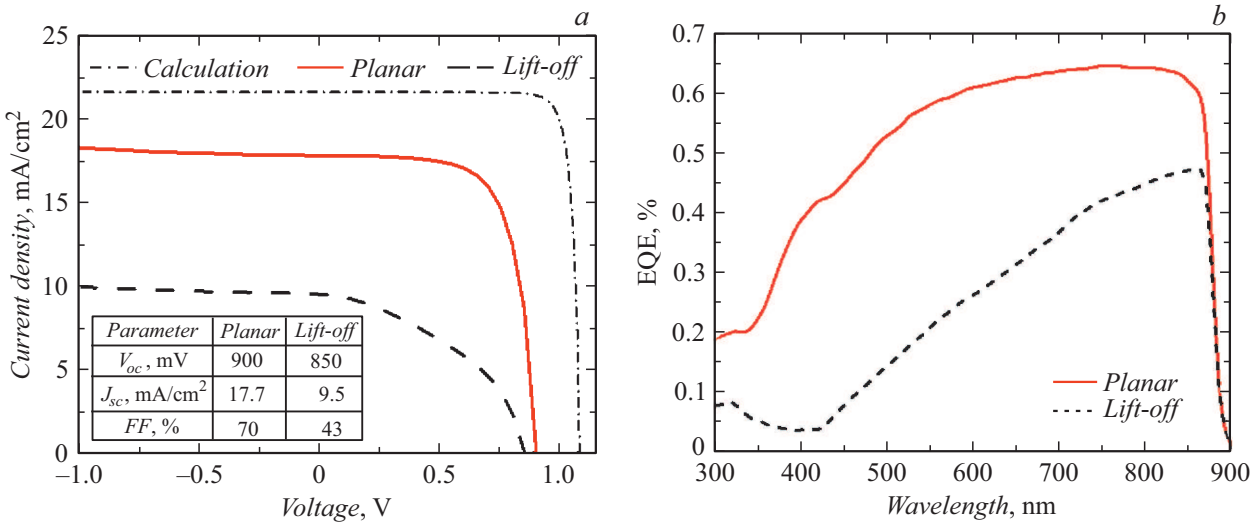

Figure 3. CVC - IV-curve under the AM1.5G spectrum (*a*) and spectrum of the external quantum efficiency (*b*) for planar and lift-off SC samples.

the contact annealing temperature. Layers of Pd/Ge/Au with a thickness of 10, 50, and 100 nm, respectively, were deposited by vacuum thermal evaporation with subsequent annealing at a temperature of 185°C for 1 h [8]. Figure 2 presents the optical image of the fabricated flexible SC on a PMMA carrier with an area of 0.3 cm^2.

Figure 3, *a* shows the SC CVCs - IV-curves measured under illumination with the standard AM1.5G solar spectrum before and after lifting off the growth substrate. The calculated CVC - IV characteristic of a model SC is also plotted for comparison. The external quantum efficiency spectra of fabricated SCs are shown in Fig. 3, *b*. The SC operation parameters before lift-off are satisfactory: open-circuit voltage $V_{oc} = 900$ mV, short-circuit current $J_{sc} = 17.7$ mA/cm^2 and fill factor $FF = 70\%$. Relatively low values of the short-circuit current and the fill factor are likely the result of formation of oval defects in the process of epitaxial synthesis [9]. The external quantum efficiency spectrum of the studied SC is characterized by a drop in the short- and medium-wave regions (up to 600–700 nm). This provides additional evidence of recombination of carriers in the emitter region. The efficiency of this cell was 11%. The short-circuit current and the fill factor decreased abruptly to 9.5 mA/cm^2 and 43% after lift-off; the open-circuit voltage did also decrease, although less significantly (to 850 mV). Compared to the planar sample, the spectral characteristics dropped additionally in the short-wave region. This is attributable to the degradation of the top wide band gap AlGaAs window in the lift-off process, which enhances the recombination of minority carriers at the interface with the emitter.

The calculated specific power (normalized to the mass of the entire cell) for the lift-off SC on a PMMA carrier 20 μm in thickness was 750 W/kg. For comparison, the value of this parameter corresponding to a carrier fabricated from aluminum foil of the same thickness is 461 W/kg [10]. Thus, the use of organic polymer carriers allows one to raise the specific power significantly.

The optimum parameters of layers of a lift-off GaAs-based SC providing the maximum efficiency of an SC of this design without an antireflective coating were determined via numerical modeling. SC heterostructures based on GaAs and AlGaAs and InAlP solid solutions were synthesized by molecular beam epitaxy. SC prototypes with thin optically transparent PMMA carriers were fabricated. The current–voltage curves and spectral characteristics of lift-off and planar SCs were measured experimentally. It was demonstrated that the use of organic polymer carriers allows one to produce SCs with a high specific power, which is especially important in the design of flexible SCs for drones and ground vehicles.

Funding

Yu.S. Berdnikov acknowledges financial support of the numerical modeling research from the Russian Science Foundation (project No. 21-79-00281).

D.M. Mitin wishes to thank the Russian Foundation for Basic Research for supporting the research into electrophysical SC properties (project 19-38-60008) and the Grant Council of the President of the Russian Federation for supporting the research into epitaxial synthesis (MK-3031.2021.1.2).

Conflict of interest

The authors declare that they have no conflict of interest.

References

[1] N. Ali, R. Ahmed, J. Luo, M. Wang, A. Kalam, A.G. Al-Sehemi, Y. Fu, Mater. Sci. Semicond. Process, **107**, 104810 (2020). DOI: 10.1016/J.MSSP.2019.104810
[2] M. Reese, S. Glynn, M. Kempe, D. McGott, M. Dabney, T. Barnes, S. Booth, D. Feldman, N. Haegel, Nature Energy, **3** (11), 1002 (2018). DOI: 10.1038/s41560-018-0258-1
[3] M. Green, E. Dunlop, J. Hohl-Ebinger, M. Yoshita, N. Kopidakis, X. Hao, Prog. Photovolt., **29** (1), 3 (2021). DOI: 10.1002/PIP.3371
[4] H.L. Chen, A. Cattoni, R. Lépinau, A.W. Walker, O. Höhn, D. Lackner, G. Siefer, M. Faustini, N. Vandamme, J. Goffard, B. Behaghel, C. Dupuis, N. Bardou, F. Dimroth, S. Collin, Nature Energy, **4** (9), 761 (2019). DOI: 10.1038/s41560-019-0434-y
[5] K. Papatryfonos, T. Angelova, A. Brimont, B. Reid, S. Guldin, P.R. Smith, M. Tang, K. Li, A.J. Seeds, H. Liu, D.R. Selviah, AIP Adv., **11** (2), 025327 (2021). DOI: 10.1063/5.0039631
[6] S. Adachi, *Properties of group-IV, III–V and II–VI semiconductors* (Wiley, 2005). DOI: 10.1002/0470090340
[7] J.W. Leem, J.S. Yu, D.H. Jun, J. Heo, W.K. Park, Solar Energy Mater. Solar Cells, **127**, 43 (2014). DOI: 10.1016/j.solmat.2014.03.041
[8] D.M. Mitin, F.Y. Soldatenkov, A.M. Mozharov, A.A. Vasilév, V.V. Neplokh, I.S. Mukhin, Nanosystems: Physics, Chemistry, Mathematics, **9** (6), 789 (2018). DOI: 10.17586/2220-8054-2018-9-6-789-792
[9] M.R. Melloch, Solar Cells, **30** (1-4), 313 (1991). DOI: 10.1016/0379-6787(91)90064-v
[10] M.A. Putyato, N.A. Valisheva, M.O. Petrushkov, V.V. Preobrazhenskii, I.B. Chistokhin, B.R. Semyagin, E.A. Emel'yanov, A.V. Vasev, A.F. Skachkov, G.I. Yurko, I.I. Nesterenko, Tech. Phys., **64** (7), 1010 (2019). DOI: 10.1134/S106378421907020X.